

# An analysis of debris-induced nonlinear phenomena in a positive ion-negative ion (PINI) plasma

Hitendra Sarkar and Madhurjya P. Bora<sup>a</sup>

*Physics Department, Gauhati University, Guwahati 781014, India*

In this work, an analysis of nonlinear waves and phenomena induced by an external charged debris in a positive ion-negative ion (PINI) plasma is presented. The process of formation of different nonlinear structures is examined theoretically through a forced Korteweg-de Vries (fKdV) equation, which is also verified with a multi-fluid flux-corrected transport (mFCT) simulation. The different processes which are responsible for different nonlinear structures excited by differently charged external debris are pointed out. This work also tries to point out the similarities in different nonlinear structures by an external charged debris (this work) and the underlying processes and those produced by a positive ion beam (other works) in a PINI plasma through beam-plasma interaction.

## I. INTRODUCTION

Nonlinear waves ubiquitously drive the dynamics of nature's most intricate systems, shaping complex phenomena from plasma instabilities to oceanic rogue waves in ways both beautiful and unpredictable. Plasma shocks and solitons remain prime examples of such structures that governs the energy transport and wave dynamics across laboratory and astrophysical environments. Solitons or solitary waves (SWs) can be considered as the localized compressions or rarefactions of plasma densities arising out of the interplay between nonlinearity and dispersion in a medium. On the contrary, shock waves (SHWs) are usually associated with some external dissipation mechanism such as kinematic viscosity, Landau damping, and collision among ions and neutrals along with inherent nonlinearity, dispersion, and weak dissipation. During a nonlinear ion-acoustic wave (IAW) propagation in a dissipative plasma, the leading edge of a propagating wave gets steepened as dissipation dominates over dispersion and a shock front is formed. In contrast to this, in a collision-less dispersive fluid, SHWs excited without dissipation often have an oscillatory signature and are known as dispersive shock waves (DSWs). Nevertheless, the nature of these nonlinear structures is largely determined by the background plasma conditions, constituents and the physical parameters associated.

The characteristics of IA solitons or SHWs excited in an usual  $e-i$  plasma are significantly different than that of a multi-ion plasma or a positive ion-negative ion (PINI) plasma. In fact, an  $e-i$  plasma can only support compressive solitons with positive electrostatic potential. However, with an addition of even a small amount of one or more extra ion species to the plasma, making it multicomponent, drastically changes the dynamics of the plasma. It is observed that in a multicomponent plasma, the IA wave propagation is mainly influenced by the lighter ions and changes in their concentrations and temperatures may lead to substantial modification of the wave structure via the plasma potential [1–3]. If the added ion species is negatively ionized, then after a critical concentration of these negative ions, the plasma potential can even change its polarity to form a negative or rarefactive soliton [2, 3]. When an ion beam is injected into such a plasma, beam-plasma interaction makes the evolution much more complex in terms of nonlinear wave structures compared to a simple plasma [3–5]. For this reason, investigations on the plasmas with negative ions as one of the constituents has always been a topic of interest. Plasmas in astrophysical and space environments such as cometary tails, planetary ionospheres, and interstellar and molecular clouds usually are inherently multi-species with two or more than two types of ions and offer a rich platform for studying a variety of wave motions with subtle intricacies [6, 7]. These multi-species plasmas with negative ions are also easily produced in a laboratory and are well studied owing to their vital role in major scientific and technological applications such as plasma processing or fusion plasmas. We believe that an investigation of nonlinear wave propagation in a PINI plasma embedded with an external charged debris is definitely a topic worth studying.

### A. Can other phenomena mimic debris-induced nonlinearities?

Effect of presence of external debris in a flowing plasma has definitely gathered attention in recent years, especially as awareness and knowledge about interaction of space debris in low-earth orbits with ionospheric plasmas have come to the forefront of space research [8–15]. Though science of detection of space debris through debris-induced plasma interaction is still quite speculative, we are definitely learning more and more about it, as research intensifies in

---

<sup>a</sup> mpbora@gauhati.ac.in

this area. In this context, we would like to raise a fundamental question about the similarities of the dynamics and structures of nonlinear waves in a plasma in general, to those induced by external charged debris. We do hope that we shall be able clear some issues about this question through the present work.

In many experiments involving beam-plasma interactions, the beam is produced *in situ*, which leaves the plasma quasi-neutral. Different nonlinear structures produced due to these interactions have interesting dynamical signatures. In such cases, if the beam velocity  $v_b$  is  $\ll v_s$ , the effective sound velocity, the propagating ion-acoustic wave (IAW) does not *see* the Debye-scale disturbances created by the beam. This is analogous to what is known as ‘plasma approximation’, which requires  $(k\lambda_D)^2 \ll 1$ , where  $k$  is the wave number of the IAW and  $\lambda_D$  is the electron Debye shielding length. We argue that so long as  $v_b$  remains considerably smaller than  $v_s$ , the plasma quasi-neutrality is maintained. However as  $v_b \sim v_s$ , the beam-plasma dynamics start getting affected by the IAW. And when  $v_b \gg v_s$ , the situation becomes quite different and the beam dynamics will be completely *detached* from the ion-acoustic dynamics. If we now consider the ion-acoustic time scale  $\tau_{IA}$ , it comes out to be  $\sim 0.01 - 0.5$  milli second for a typical laboratory device. On the other hand, the electron-ion collision time  $\tau_{ei}$  is quite large  $\sim 5$  millisecond for such parameters. As a result, when  $v_b \gg v_s$ , there is no way that thermalization can occur between the beam and the background plasma and the background plasma should *see* the beam as an external charged perturbation (debris) and the beam-plasma dynamics should closely mimic the dynamics observed in plasma-debris interaction. In subsequent sections, we show that this is indeed true and can be proven quite reasonably. We also see similarities among the nonlinear structures produced by externally induced perturbation in plasma to that of debris-induced perturbation. In this regard debris-induced perturbations can be thought to be quite commonplace in many experimental arrangements.

In this work, we explore different nonlinear structures excited by a moving charged debris in a multicomponent PINI plasma and also look at the similarities of their characteristics with experimental results. The complete plasma system is modeled using a forced Korteweg–de Vries (fKdV) equation and results from theoretical analysis were verified using a 1-D multi-fluid flux-corrected transport (mFCT) simulation [13]. The paper is organized as follows. The detailed plasma model and the governing equations are described in Sec. II. Sec. III contains the description of fKdV dynamics and interpretation of its results. In Sec. IV results from FCT simulation were presented, Sec. V briefly addresses the variation of nonlinearity with debris velocity and in Sec. VI, we conclude.

## II. PLASMA MODEL AND GOVERNING EQUATIONS

The model we are going to consider is a 1-D warm positive ion-negative ion (PINI) plasma with an external charge debris embedded into it. The relevant equations are the continuity and momentum equations for positive and negative ions. The equations are closed by the Poisson equation. The electrons are considered to be Boltzmannian. The equations are given by

$$\frac{\partial n_{\pm}}{\partial t} + \frac{\partial}{\partial x}(n_{\pm}v_{\pm}) = 0, \quad (1)$$

$$n_+ \frac{dv_+}{dt} = -\sigma \frac{\partial n_+}{\partial x} - n_+ \frac{\partial \phi}{\partial x}, \quad (2)$$

$$n_- \frac{dv_-}{dt} = -\frac{\sigma}{\mu} \frac{\partial n_-}{\partial x} + \frac{n_+}{\mu} \frac{\partial \phi}{\partial x}, \quad (3)$$

$$\frac{\partial^2 \phi}{\partial x^2} = n_e - \delta n_+ + (\delta - 1)n_- - \rho_{\text{ext}}, \quad (4)$$

where  $(n_{\pm}, v_{\pm})$  are respectively positive and negative ion densities and velocities,  $\phi$  is the plasma potential. The quantity  $\sigma = T_i/T_e$  is the ratio of ion temperature to that of the electrons. Here, we have taken the temperatures of positive and negative ions to be equal  $T_i = T_+ = T_-$ . The mass ratio of negative to positive ions is denoted by  $\mu = m_-/m_+$  and  $\delta = n_{+0}/n_{e0}$  is the ratio of the equilibrium positive ion density to the equilibrium electron density. In order to be able to compare our analytical results with existing laboratory experiments, we have assumed  $m_+ > m_-$ , which is mostly the case in case of experiments [2–5, 16]. In the above equations, the densities are normalized by their respective equilibrium values and potential is normalized by  $(T_e/e)$ . Time is normalized by  $\omega_i^{-1}$ , with  $\omega_i = \sqrt{n_{e0}e^2/(m_+\epsilon_0)} \equiv \delta^{-1/2}\omega_{p+} \equiv (\delta - 1)^{-1/2}\omega_{p-}$ , where  $\omega_{p\pm}$  are the respective positive ion and negative ion plasma frequencies. While length is normalized by electron Debye length, velocities are normalized by the ion sound speed  $c_s = \sqrt{T_e/m_+}$ , as determined by the mass of the heaviest species. The quantity  $\rho_{\text{ext}} \equiv \rho_{\text{ext}}(x - v_d t)$  is the normalized charge density of the external debris with  $v_d$  as the normalized velocity of the external debris. The overall charge neutrality of the PINI plasma without external debris is ensured through the relation

$$n_{e0} + n_{-0} = n_{+0}. \quad (5)$$

The normalized electron density is given by  $n_e = e^{\phi}$ .

### A. The morphology of debris-induced nonlinearities

Before we investigate the nonlinear waves and structures induced by a charged debris in a PINI plasma, it is of relevance to discuss a bit about the fundamental physics of these nonlinearities in an  $e$ - $i$  plasma. We now know that the response of an  $e$ - $i$  plasma to an embedded charged debris very well depends on the nature of the charge of the debris [13]. It has been *only* recently shown that the formation of bright pinned solitons in the ion-acoustic regime due to the presence of a negatively charged debris is basically a manifestation of the trapped ions in phase-space vortices formed due to ion-ion counter streaming instability (IICSI) [15]. Besides, proper spatial resolution of the pinned solitons requires a certain relative velocity between the debris and the plasma, though higher relative velocities may cause the pinned solitons to disappear [10, 15]. In contrast, a positively charged debris creates an ion hole, exciting an ion-acoustic wave (IAW), which propagates away from the site of the debris. However, when there is a relative motion between the debris and the plasma, the IAW becomes a dispersive shock wave (DSW) in the precursor region [13].

Following the above explanation, we expect that the response of a PINI plasma to external charged debris should also be characteristically different for positively and negatively charged debris. We further expect that for  $\delta \sim 1$ , the response should be similar to that of an  $e$ - $i$  plasma.

### III. FORCED-KDV DYNAMICS

We shall now see, what forced-KdV (fKdV) dynamics has to offer. The fKdV equation is derived using the usual reductive perturbation theory by using the following expansions, assuming a static and neutral equilibrium. The external charged debris is introduced as a second order perturbation. The expansions are

$$n_{\pm} \simeq 1 + \varepsilon n_{\pm}^{(1)} + \varepsilon^2 n_{\pm}^{(2)} + \dots, \quad (6)$$

$$v_{\pm} \simeq \varepsilon v_{\pm}^{(1)} + \varepsilon^2 v_{\pm}^{(2)} + \dots, \quad (7)$$

$$\phi \simeq \varepsilon \phi^{(1)} + \varepsilon^2 \phi^{(2)} + \dots, \quad (8)$$

$$\rho_{\text{ext}} = \varepsilon^2 \rho_{\text{ext}}^{(2)}, \quad (9)$$

where  $\varepsilon$  is the expansion parameter, which is  $\ll 1$ . We now use the stretched variables  $\xi = \varepsilon^{1/2}(x - Vt)$  and  $\tau = \varepsilon^{3/2}t$  for space and time coordinates, where  $V$  is the dimensionless phase velocity of the IAW. Following the usual procedure, by collecting the first order terms, we have the following expressions for the first order variables in terms of  $\phi^{(1)}$ ,

$$n_+^{(1)} = \frac{\phi^{(1)}}{V^2 - \sigma}, \quad (10)$$

$$n_-^{(1)} = -\frac{\phi^{(1)}}{V^2\mu - \sigma}, \quad (11)$$

$$v_{\pm}^{(1)} = Vn_{\pm}^{(1)}, \quad (12)$$

where the phase velocity expression (or the compatibility condition) is given by

$$V = \left[ \frac{\alpha + \sqrt{\alpha^2 - 4\mu\sigma(2\delta + \sigma - 1)}}{2\mu} \right]^{1/2}, \quad (13)$$

with  $\alpha = (\mu + 1)(\delta + \sigma) - 1$ . Collecting the next higher order terms and eliminating the second order quantities, using the Poisson equation, we finally get the fKdV equation as follows

$$\partial_{\tau}\phi^{(1)} + A\phi^{(1)}\partial_{\xi}\phi^{(1)} + B\partial_{\xi}^3\phi^{(1)} = -B\partial_{\xi}\rho_{\text{ext}}^{(2)}, \quad (14)$$

where nonlinear and dispersion coefficients  $A$  and  $B$  are given by

$$A = \left[ \frac{(b + 2V^2)\delta}{b^3} - \frac{2(\delta - 1)V^2\mu}{a^3} - \frac{(\delta - 1)}{a^2} - 1 \right] B, \quad (15)$$

$$B = \left[ 2V \left\{ \frac{(\delta - 1)\mu}{a^2} + \frac{\delta}{b^2} \right\} \right]^{-1}, \quad (16)$$

and  $a = (V^2\mu - \sigma)$  and  $b = (V^2 - \sigma)$ .

We note that unlike the KdV equation, the fKdV equation, in general, is non-integrable and has to be solved numerically. In what follows, we present the numerical solutions of Eq.(14) for a Gaussian charge density profile for the external debris with periodic boundary conditions.

### A. Numerical results

We now present the results representing nonlinear structures in a flowing PINI plasma with an embedded external charged debris, as obtained from the numerical solution of the fKdV equation given by Eq.(14). What we shall observe is the appearance of dark pinned solitons as debris velocity becomes supersonic when the debris charge is positive. In what follows, we shall discuss two other experimental cases (*i*) PINI plasma with a positive ion-beam and (*ii*) large-amplitude perturbation in a PINI plasma, for which we shall try to draw a parallel between the nonlinear oscillations for a PINI plasma with external charged debris (this study) and these experimental cases. All the figures in the subsequent sections are drawn in the rest frame of the debris. We present our results with respect to two independent parameters –  $\delta$  and  $v_d$  for a fixed  $\sigma$ .

#### 1. Perturbation with positively charged external debris

The first set of results shown in Fig.1 are for debris with a positive charge  $\rho_{\text{ext}} > 0$  at the end of  $\tau = 100$  with  $\sigma = 0.1$ . The figure shows the nonlinear waves in  $\phi \equiv \phi^{(1)}(\xi, \tau)$ . The charge density distribution of the debris is a Gaussian-shaped distribution  $\rho_{\text{ext}}(\xi) = \rho_0 e^{-\xi^2/\Delta}$ , where  $\rho_0$  is the peak of the distribution and width is determined by  $\Delta$ . We note that the external debris is introduced as a perturbation with  $\rho_0$  denoting the strength. In all the cases (unless indicated otherwise), we have used a perturbation with  $\rho_0 = 0.5$  which is equivalent to a perturbation  $\equiv 50\%$  of the equilibrium density. In the figure, the shaded region shows the extent of the debris charge distribution centered in the middle of the frame indicated by the dashed vertical line. The debris move with a velocity  $v_d$  from right to left. In Fig.1, we observe that for low (subsonic)  $v_d$  (top left panel of Fig.1), the debris excites bright IA solitons which move away from the debris in the precursor region. We also observe that the velocities of these IA solitons increase from being subsonic to becoming supersonic as  $\delta$  increases from 1.02 to 1.8. We also note that in the production of a PINI plasma, experimentalists usually use an electronegative gas in an  $e-i$  plasma to create negative ions at the expense of less warm electrons and an increase of  $\delta$  causes an increase in negative ion density in a PINI plasma. So, the increase of velocity of the IA soliton is due to the increase in negative ion density. However, as debris velocity increases and becomes sonic, higher  $\delta$  perturbations slow down in comparison to lower  $\delta$  perturbations which ultimately forms dark pinned solitons as debris velocity increases more as shown in the three panels on the right in Fig.1. As  $v_d$  increases, pinned solitons tend to form at the debris position for higher  $\delta$  whereas low  $\delta$  perturbations never get to form pinned solitons and remain predominantly a positive nonlinearity in the form of a DSW in the precursor region.

These results are entirely in conformity with what we know about formation of debris-induced pinned solitons and DSWs. We now know that in an  $e-i$  plasma the pinned solitons formed due to moving negatively charged debris is basically a manifestation of the ions trapped in the phase space vortices formed by the IICSI [15], whereas a positively charged debris induces a DSW in the precursor region. So, for  $\delta \sim 1$  (very less concentration of negative ions), the plasma behaves like the usual  $e-i$  plasma and no pinned solitons can form for a moving positively charged debris. However for  $\delta > 1$ , the negative ions are attracted by the positively charged debris causing a IICSI-like phenomena for negative ions, leading to formation of phase space vortices which in turn cause formation of dark pinned solitons at the debris position.

#### 2. Comparison with ion-beam dynamics in a PINI plasma

Let us now discuss the case for a positive ion-beam dynamics in a PINI plasma, where the positive ion-beam is produced in situ by accelerating a part of the ion population in the plasma so that overall quasi-neutrality is maintained throughout [3]. This case is interesting as there are several investigations being carried out by different authors to analyze the formation of nonlinear structures in such plasmas [4, 5].

Let us consider such a three-component PINI plasma, consisting of positive ion ( $n_+$ ), negative ion ( $n_-$ ), and electron ( $n_e$ ), in the presence of a positive ion beam ( $b^+$ ), as considered in the experimental work by Nakamura [3] (N99 hereafter). Note that the whole system is to be considered quasi-neutral,

$$n_+ + n_{b^+} = n_- + n_e = n_T, \quad (17)$$

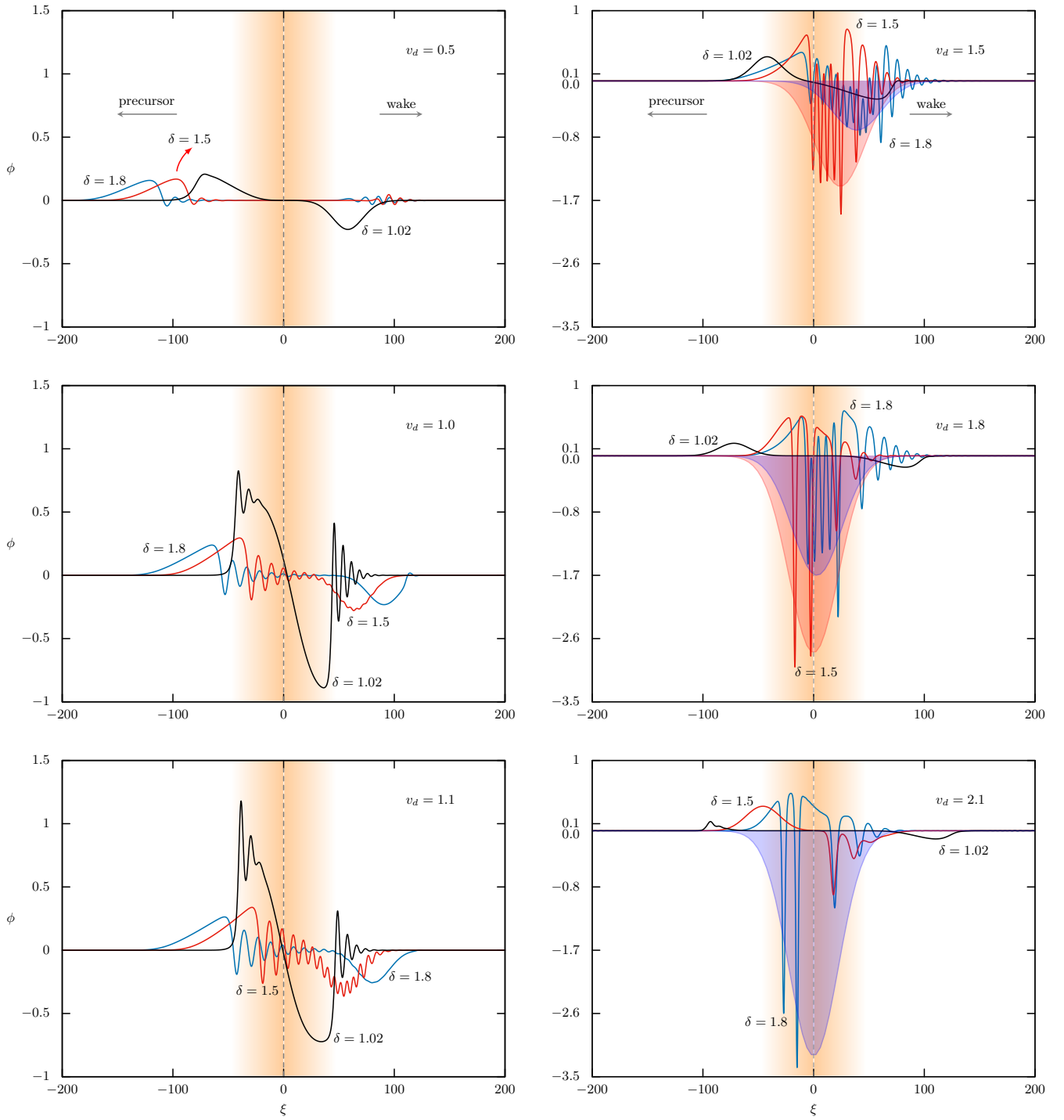


Figure 1. Nonlinear wave for a flowing plasma with a positively charged external debris. All panels are drawn in the rest frame of the debris, which is in the middle of a panel, denoted by a vertical dashed line. The shaded vertical regions indicate the extent of the charged debris. The shaded envelopes on the right hand panels indicated the envelopes of the corresponding dark pinned solitons.

which essentially requires that the positive ion beam to be created in situ. As a result, the formation of the positive ion beam requires an overall depletion of the bulk positive ions. The comparative concentration of negative ion is denoted by the quantity  $r = n_-/n_T$ , which can be written in terms of  $\delta$

$$\delta = \frac{1}{1 - r}. \quad (18)$$

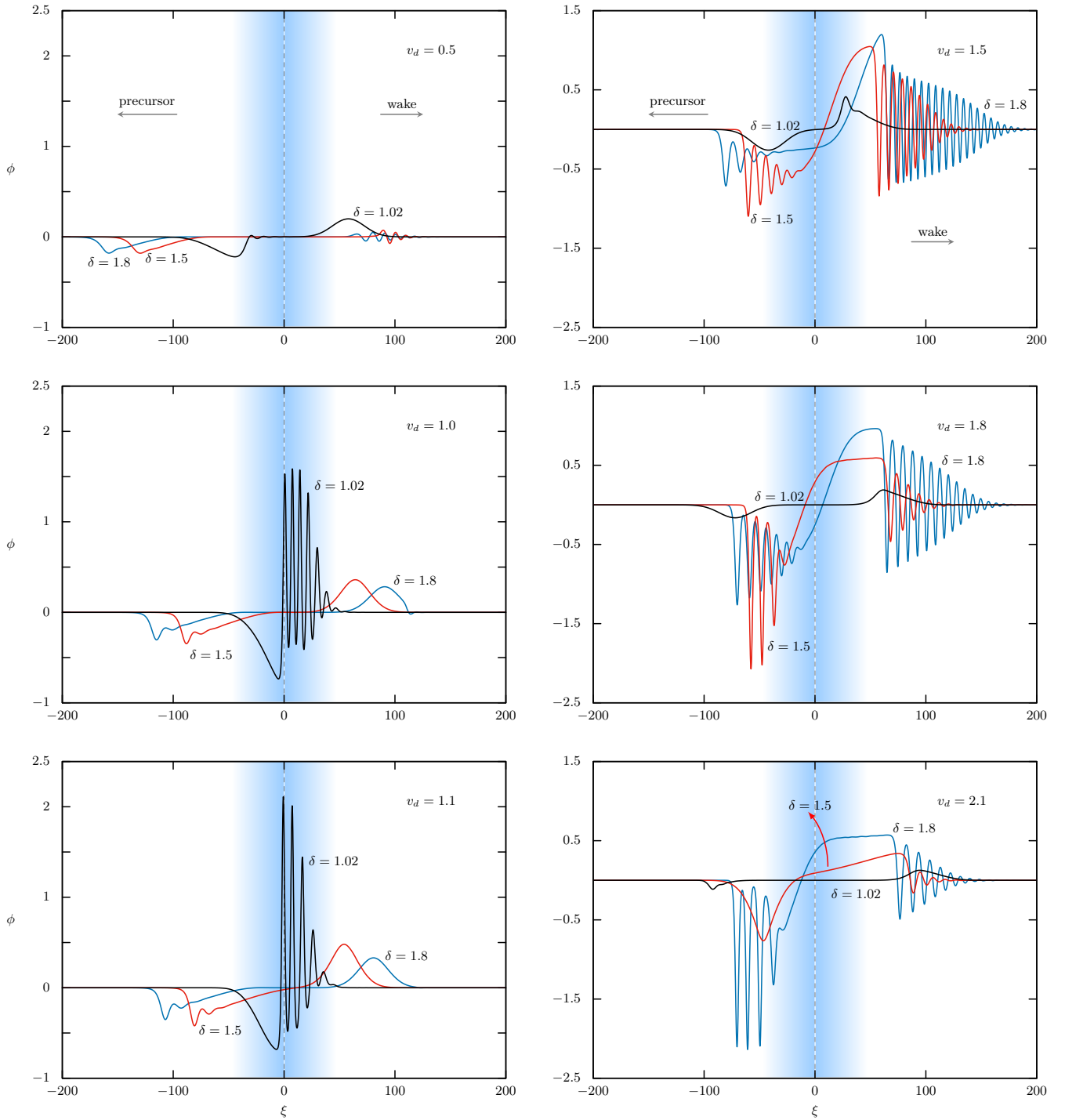


Figure 2. Nonlinear wave for a flowing plasma with a negatively charged external debris. All other particulars are same as in Fig.1. The shaded vertical regions indicate the extent of the negatively charged debris.

Let us now consider the slowest possible ion-acoustic time scale which is given by

$$\tau_{IA} = f^{-1} = \left[ \frac{k}{2\pi} \sqrt{\frac{T_e}{m_+}} \right]^{-1}, \quad (19)$$

where  $k = 2\pi/\lambda$  with  $\lambda$  being the wavelength of the ion-acoustic wave. In the above expression  $T_e$  is the electron temperature which  $\sim 1$  eV and  $m_+$  is the mass of the heaviest ion, which is  $\text{Ar}^+$ , so that  $m_+ \sim 40m_p$ , where  $m_p$  is

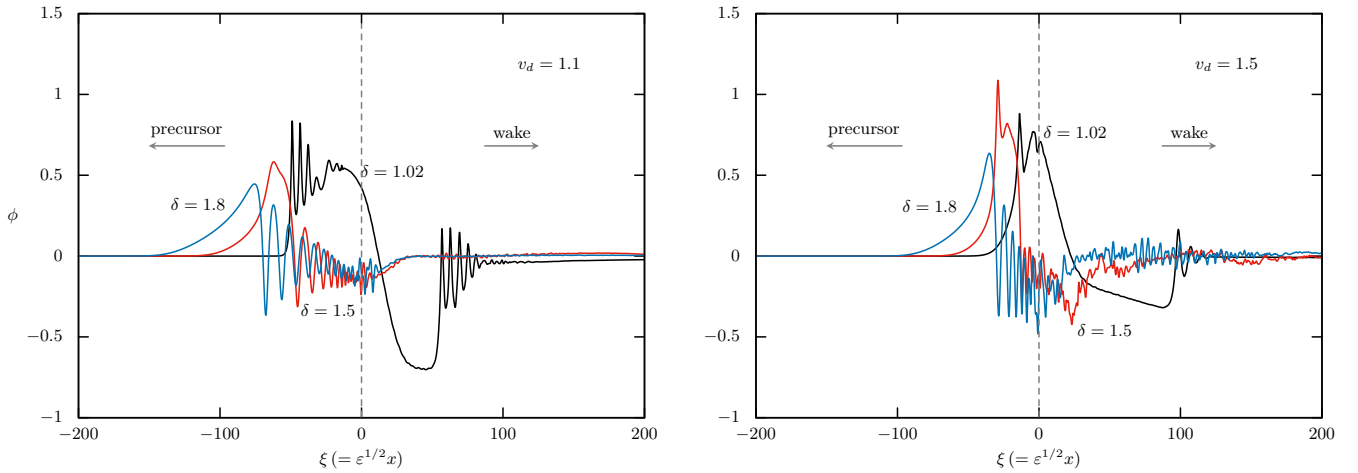


Figure 3. FCT simulation results of propagation of nonlinear wave in a PINI plasma with and embedded external positively charged debris. These results are equivalent to the theoretical cases obtained through fKdV solution shown in Fig.1. The left panel in the above figure corresponds to the left-bottom panel of Fig.1 and the right panel above corresponds to the right-top panel of Fig.1. These results are plotted at the end of  $\tau = 100 \equiv \varepsilon^{3/2}t$ .

the mass of a proton. Assuming the experimental double-plasma device to be of length  $\sim 90$  cm [3], we can assume the largest possible ion-acoustic wavelength to be  $\sim 0.45$  m. With these parameters, we have  $\tau_{IA} \sim 0.03$  milli second. If we now consider the electron-ion collision time  $\tau_{ei}$ , we have

$$\tau_{ei} = \frac{6\sqrt{2}\pi^{3/2}\epsilon_0^2 m_e^{1/2} T_e^{3/2}}{n_e e^4 \ln \Lambda}, \quad (20)$$

where  $\ln \Lambda$  is the Coulomb logarithm  $\sim 10 - 12$ . For  $n_e \sim 10^7 \text{ cm}^{-3}$  [3], we have  $\tau_{ei} \sim 3.5$  milli second. We now argue that as  $\tau_{ei} \gg \tau_{IA}$ , we can safely assume that in the ion-acoustic timescale, the plasma will not be able to thermalize. As a result a positive ion beam propagating through the plasma, the positive ions of the beam will not be able to thermalize with the bulk plasma and for all practical purpose, the beam will behave as an external debris. It has been observed in N99 that below a certain critical value for beam velocity, increasing  $r$  (higher  $\delta$ ) causes the nonlinearity to become negative from positive. However, beyond the critical value of the beam velocity, the nonlinearity remains positive irrespective of the initial pulse (which is reported only at higher  $\delta$  in N99). In our case as well, we see a similar behavior as evident from the panels in the left column of Fig.1. We can see that when debris velocity is  $\lesssim 1.1$ , for low  $\delta$  ( $\sim 1$ ), there is a steepening in the leading edge indicating positive nonlinearity while for higher  $\delta$ , the steepening is on the falling edge, which indicates negative nonlinearity. We note that the ‘positive nonlinearity’ in the case of a compressive or bright soliton is referred with respect to the nonlinear term  $A\phi^{(1)}\partial_\xi\phi^{(1)}$  [see Eq.(14)] in a usual KdV equation (without the debris term), which is responsible for steepening of the leading edge of a soliton. On the other hand, when the steepening occurs in the falling edge, it is usually termed as ‘negative nonlinearity’. When debris velocity increases (bottom right panel of Fig.1), the negative nonlinearity which was observed for say  $\delta = 1.5$  and with low  $v_d$ , decreases and get balanced by dispersion giving rise to a bright KdV soliton. These results are also confirmed through FCT simulation, which are being presented in another subsection.

We should however be cautious not to compare the entire experimental results of N99 with the results obtained in this work, as the external charged debris in this work is a localised charged perturbation with no assumption of quasi-neutrality, while in N99 and other similar experimental works, the beam is an extended structure with definitive wake region. So, we can probably compare only the leading edge dynamics of a beam-plasma interaction with the precursor region of debris-induced nonlinearity.

### 3. Comparison with external perturbation in a PINI plasma

Let us now consider a very recent experimental observation of large-amplitude perturbation in a PINI plasma by Pathak and Bailung [16] (P25 thereafter), where a positive pulse is induced externally to a PINI plasma resulting a large-amplitude positive perturbation (up to 70% of equilibrium plasma density), which is then used to study the effect of controlled Landau damping on nonlinear IA wave. This produces a dissipative shock front when dissipation

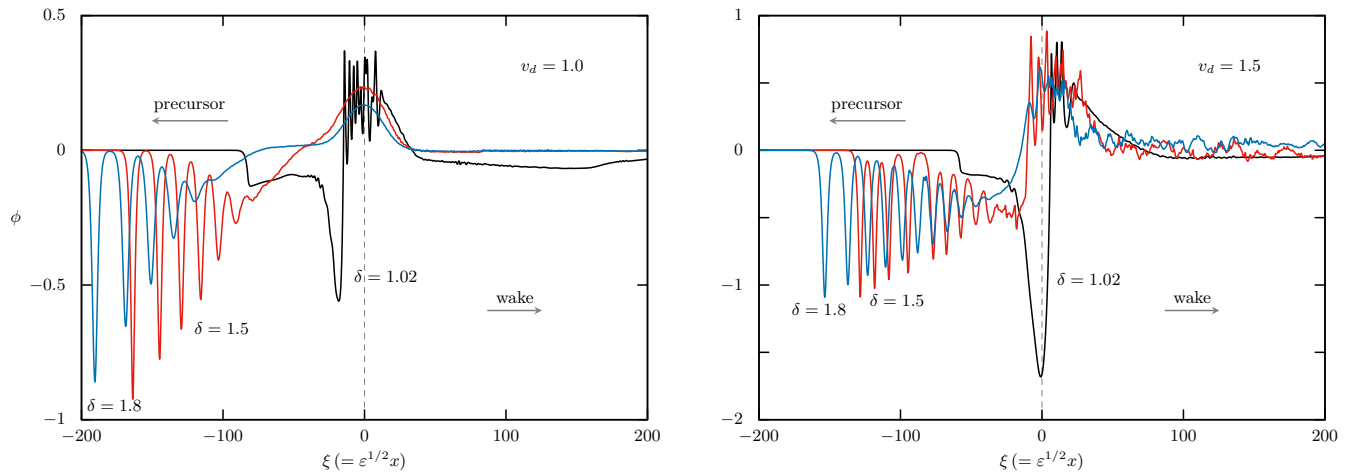


Figure 4. FCT simulation results of propagation of nonlinear wave in a PINI plasma with and embedded external negatively charged debris. These results are equivalent to the theoretical cases obtained through fKdV solution shown in Fig.1. The left panel in the above figure corresponds to the left-middle panel of Fig.2 and the right panel above corresponds to the right-top panel of Fig.2. These results are plotted at the end of  $\tau = 100 \equiv \varepsilon^{3/2}t$ .

(through Landau damping) becomes large.

We argue that dynamically, an external perturbation can be considered to be having the same effect as an external charged debris so far as the leading edge (or precursor region) is concerned. So, we can expect a similar behavior of nonlinear wave front for this external perturbation and perturbation induced by an external debris. In this context, we would like to compare our results as shown in the cases for  $\delta = 1.02$  with  $v_d = 1.0, 1.1$  (two bottom panels of the lefthand column in Fig.1) in the precursor regions and the case shown in Fig.4 of P25, which is comparable to our theoretical situation. In both cases, we have a leading shock front with oscillations which are nothing but dispersive shock wave (DSW) when there is no dissipation. Note that Fig.4 of P25 is for the case when Landau damping is negligible with negligible negative ions ( $\delta \sim 1.0$ ). The situation is however different in the wake region (or trailing region of the pulse). This is due to the fact that experimentally a one-time external perturbation is induced by pushing a signal which then propagates in the form of discontinuity (either as a single soliton as a ramp structure) through the plasma which then transforms into a DSW as it moves. For the case of external debris however, the perturbation remains intact all throughout the life cycle of the nonlinear wave front giving rise to a very definitive signature in the wake region.

#### 4. Perturbation with negatively charged external debris

We now present the results for a negatively charged debris in a flowing PINI plasma in Fig.2. All the parameters are kept same as in the case for positively charged debris. The shaded regions in all the panels show the extent of the charged debris with the centered dashed line indicating the debris position. As expected, bright pinned solitons are formed for  $\delta$  close to unity at  $\delta = 1.02$ , when the relative velocity between debris and PINI plasma  $v_d$  exceeds a certain value (left-top and middle panels of Fig.2). It can be clearly seen that as  $v_d$  increases, these pinned solitons finally vanishes even for  $\delta \rightarrow 1$ . For higher values of  $\delta$ , IA waves in the precursor region propagate showing an oscillatory shock excitation which is not fully formed at a lower debris velocity. However, as  $v_d$  increases amplitude of the precursor wave-front also increases and fully developed DSWs are observed to be formed. Here, it is worth mentioning that, similar behavior was also reported for the propagation of a rarefactive pulse in presence of positive ion beam in high negative ion density plasma [5]. Increasing the beam velocity resulted in a rise in soliton amplitude and a knee formation at the downstream, culminating in the formation of a shock-like structure. A realistic fluid simulation for much longer time period shows that these DSWs, as they propagate away from the site of the debris, get transformed into a train of *individual* solitons after segregation of the peaks, about which we shall discuss in Sec.IV (Fig.5). The pinned solitons at the site of the debris are deformed due to the presence of the shock. Also, behind the debris, soliton-like structures are seen to be excited due to IA oscillations.



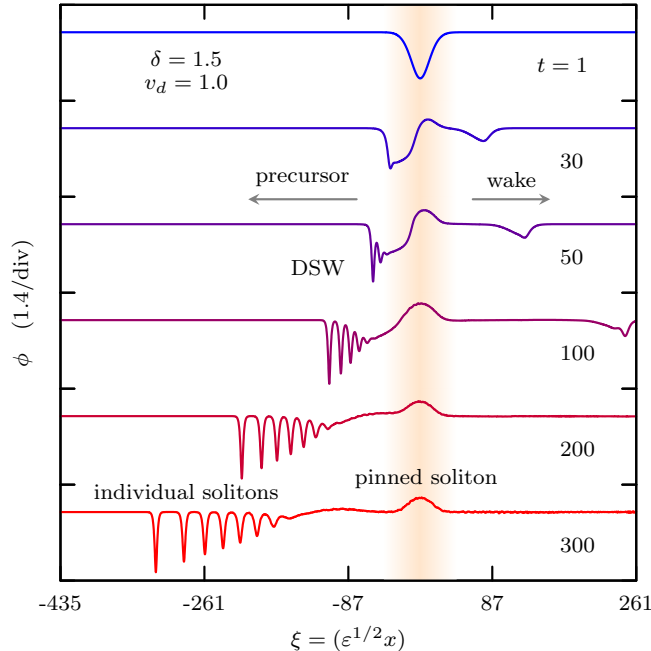


Figure 5. FCT simulation results showing evolution of a DSW in the precursor region over time for a negatively charged debris perturbation. Shaded region corresponds to the perturbation site.

#### IV. FLUX-CORRECTED TRANSPORT (FCT) SIMULATION

To corroborate the above theoretical analysis, we now present an FCT simulation of the PINI plasma with an embedded external charged debris. We use a 1-D multi-fluid FCT (*m*FCT) code [13] based on Boris's original algorithm [17] with Zalesak's flux limiter [18]. The FCT formalism requires the hydrodynamic equations Eq.(1-3) to be put in the form of a generalized continuity equation,

$$\frac{\partial f}{\partial t} = -\frac{\partial}{\partial x}(fv) + \frac{\partial s}{\partial x}, \quad (21)$$

where  $f = (n_+, n_-, n_+ v_+, n_- v_-)$  is the physical quantity to be solved,  $(fv)$  is the corresponding flux, and  $s$  is the source term. The external charged debris is entered through the Poisson equation Eq.(4) as before which is to be solved at every time step along with Eq.(21). Our FCT simulation results are presented through Fig.3 for the case with positively charged debris and through Fig.4 for negatively charged debris. In Fig.3, we have shown the results of the *m*FCT simulation for the cases shown in the left-bottom panel of Fig.1 (corresponding to the left panel of Fig.3) and right-top panel of Fig.1 (corresponding to the right panel of Fig.3). These curves are plotted at the end of  $\tau = 100 \equiv \varepsilon^{3/2}t$ . The  $x$ -axis is also respectively scaled for  $\xi \equiv \varepsilon^{1/2}x$ . Our estimate shows that the effective  $\varepsilon \sim 0.7$  for  $\rho_0 = 0.5$ , which is used in the fKdV solution as well as in the *m*FCT simulation. In both cases, the external charged debris is a Gaussian profile given by  $\rho_{\text{ext}}(\xi) = \rho_0 e^{-\xi^2/\Delta}$ .

We now present the results of FCT simulation for negatively charged debris in Fig.4. All other parameters except the debris charge is same as in the case of Fig.3. The left panel of Fig.4 corresponds to the fKdV solution presented in left-middle panel of Fig.3 and the right panel corresponds to the right-top panel of Fig.3. Though the bright pinned solitons for  $\delta = 1.02$  is properly captured in the FCT simulation, DSWs for higher  $\delta$  is shown in both  $v_d = 1.0$  and  $1.5$ , while in fKdV solutions, only in the case of  $v_d = 1.5$ , these DSWs seem to appear fully formed. Besides, the distinct soliton-like structures in the wake regions present in the fKdV solutions for both cases seem to absent in the simulation. Instead, singly peaked pinned solitons with almost no wake oscillations for  $v_d = 1.0$  and peak-modulated pinned solitons [10] and a turbulent wake trail due to the propagating shock for  $v_d = 1.5$  are found to exist. These discrepancies between the fKdV solution and FCT simulations perhaps can be attributed to the weak nonlinearity approximation that is in-built in fKdV derivation, while in FCT simulation there is no approximation on nonlinearities involved. As a result, nonlinear oscillations and structures tend to be more prominent in the simulation. Nevertheless, we believe that to large extent the fKdV dynamics is similar to the FCT simulations and our observations about similarities between

debris-induced nonlinearities and nonlinearities introduced by positive ion-beam and large-amplitude perturbation in a PINI plasma can be fairly ascertained.

It is important to note that the DSWs seen in Fig. 2 and 4 are called ‘quasi-steady state shocks’ [19] as the initial oscillatory shock profile is not retained over a longer time period ( $t \geq 200$ ). Fig.5 shows the potential distribution of one such shock profile at different time-steps ( $t = 0 - 100$ ). Initially, the external charge perturbation introduces a highly nonlinear IA wave and the leading edge of the precursor becomes steepened which forms a DSW with an oscillatory tail behind due to its dispersive nature. This non-steady shock profile, after a relatively long time ( $t \geq 200$ ), transforms into a train of individual propagating solitons as nonlinearity gets balanced by dispersion and each and every oscillatory peaks in the DSW separates into individual soliton structures. This effect is already observed and confirmed by earlier investigations on IA shock waves both in theory and experiments [19]. The positive hump observed at the site of the debris is the signature formation of a single-peak bright pinned soliton.

## V. DEBRIS VELOCITY AND NONLINEARITY

One very interesting phenomenon is the changing property of the nonlinearity with increasing debris velocity which is similar to what is observed experimentally with respect to beam velocity in a PINI plasma [4]. What we observe is that as debris velocity increases, the wave amplitude steadily increases until reaching a maximum and then decreases, which is seen from the steepening in the leading edge (precursor region), which then gradually changes to a DSW before becoming a train of solitons and then a single KdV soliton. While the steepening in the leading edge indicates a dominant positive nonlinearity over dispersion at low debris velocity, as debris velocity increases, nonlinearity decreases and gets balanced by dispersion which creates a KdV soliton. In Fig.6, we show this effect as obtained from the fKdV solution (left column) and from  $m$ FCT hydrodynamic simulation (right column). In this figure, we have indicated the changing nonlinearity with an arrow with the keywords ‘steepening’, ‘DSW’, ‘train’, and ‘KdV’, respectively to indicate the phenomenon of steeping in the leading edge, formation of DSW, transformation to a train of solitons, and finally a simple KdV soliton as debris velocity  $v_d$  increases from 0.8 to 1.5 for fKdV solutions and from 0.3 to 1.8 for  $m$ FCT solutions. All the panels are drawn at the rest frame of the debris, which is moving toward left. The thick, gray colored pulse in each frame indicates the early stage of the perturbation induced by the moving debris which has later transformed. It is important to note that all these evolutions are drawn at the same time evolution (column wise) across different  $v_d$ . The parameters are slightly different for fKdV and  $m$ FCT solutions which are optimized respectively to represent this effect. This parameter difference of fKdV and  $m$ FCT solutions can be attributed to the weak nonlinearity approximation that is inherent in the KdV formalism and full hydrodynamic simulation through FCT simulation.

We should also note that all these nonlinearities change their behaviors as the plasma evolves in time. So, for example, a steepening event of the ledge edge will eventually transform itself into another form as we evolve the system in time. This is also evident from the similar experimental observations [4, 5]. In this context we would like to recall that a pure KdV equation is integrable with ‘sech’ solution which *does not* get evolved in time. However, an fKdV equation is inherently non-integrable and different nonlinear solutions of the fKdV equation such as DSW or pinned solitons are necessarily transient phenomena and are bound to evolve in time. As per the parameters used in the FCT simulation, assuming an equilibrium plasma number density of  $\sim 10^6 \text{ cm}^{-3}$ , the entire spatial nonlinear evolution frame shown in Fig.6 is contained within  $\sim 25 \text{ cm}$ , which is quite comparable to distance over which these phenomena are observed in contemporary plasma devices [4, 5].

## VI. SUMMARY AND CONCLUSION

To summarize, we have presented a detailed study of external debris-induced nonlinear structures in a multicomponent positive ion-negative ion (PINI) plasma. The motivation to choose a PINI plasma for this study is primarily due the fact that PINI plasmas are easily produced in low-temperature laboratory devices and also are widely used in plasma processing experiments. On the other hand, theoretical and experimental (laboratory and also space-based) studies of debris-induced nonlinear plasma phenomena have been recently generating a lot of interests among the plasma physicists, especially due to the renewed attention of the scientific community in detection and removal of space-debris from low-earth orbits. Besides a detailed analysis of nonlinear waves excited by external charged debris, we also point out the similarities in certain characteristics with those excited by a high velocity positive ion beam or large amplitude perturbations in such plasmas. The important findings of our analysis are presented below.

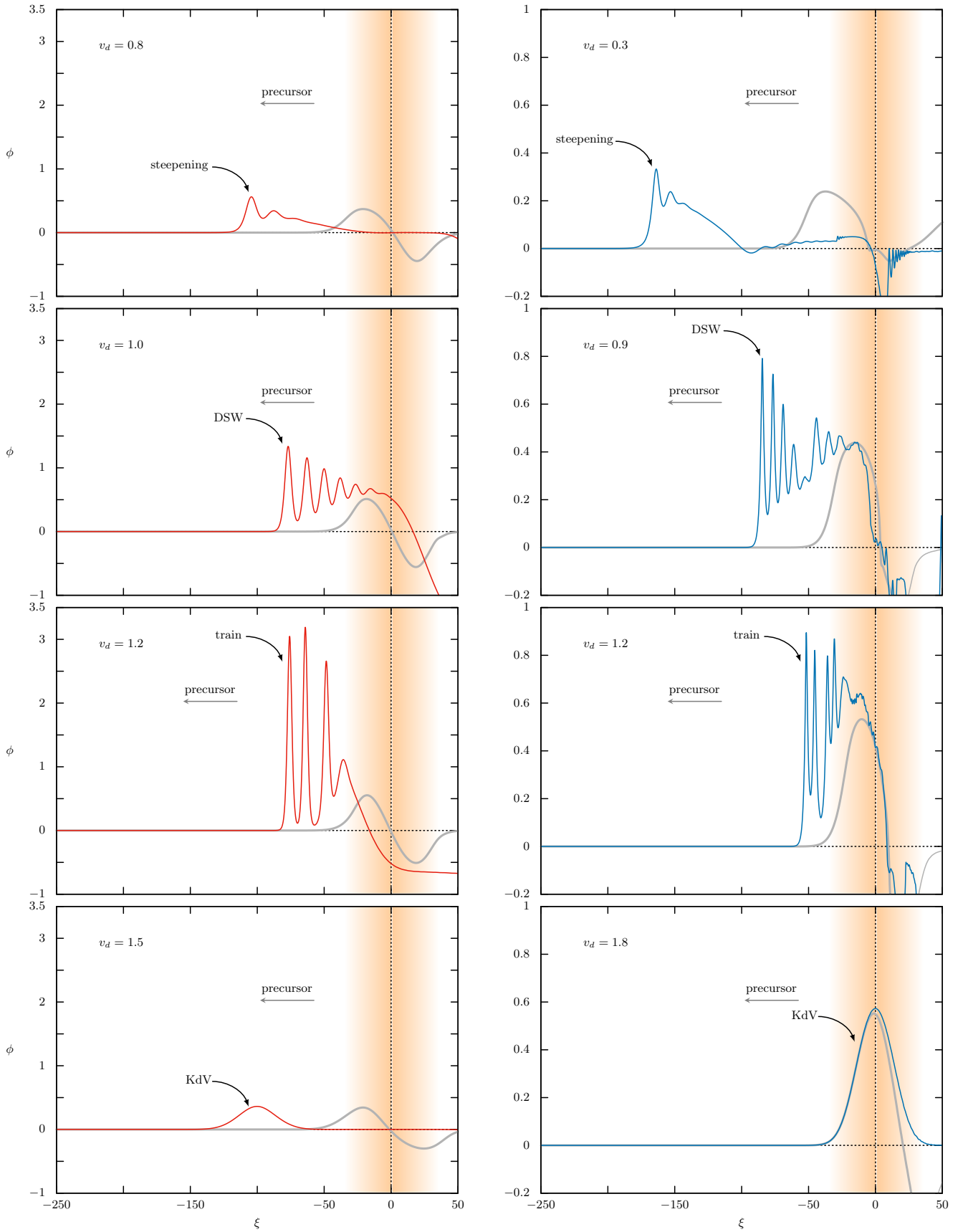


Figure 6. The changing nonlinearity with increasing debris velocity (from top to bottom) as obtained from the fKdV solutions (left column). The shaded region in each panel indicates the extent of the debris centered at  $\xi = 0$ . The thick, gray pulse in each frame is the debris-induced perturbation at the early stage of the evolution which has later transformed into their respective form as time progresses. The mFCT simulation results are in the right column. Density ratio ( $\delta$ ) and ion to electron temperature ratio ( $\sigma$ ) are taken to be 1.05 and 0.05 respectively.

*Debris-induced nonlinear waves*

- For positively charged debris moving with subsonic velocities, small amplitude bright solitons are observed with steepening in the leading edge in low  $\delta$  (low negative ion density) plasmas. On the other hand, steepening starts on the falling edge of the wave as  $\delta$  is increased beyond certain value and as debris velocity reaches sonic and supersonic regime, large amplitude dark pinned solitons are excited. However, for the same velocity regime, DSWs are seen to be formed in low  $\delta$  plasma. At very high debris velocity, the precursor wave is found to transform into a KdV like soliton.
- On the contrary, for perturbation induced by a negatively charged debris, the nature and morphology of nonlinear structures are exactly opposite to what is observed in the case of positively charged debris. Presence of higher concentration of negative ion species (high  $\delta$ ) leads to formation of quasi-static DSWs as debris velocity becomes supersonic and bright pinned solitons are formed in the presence of lower concentration of negative ions (low  $\delta$ ). However, the nature of nonlinearity of the excited waves remains the same as in the case of a positive debris perturbation.
- Toward the end, we have also shown how the KdV nonlinearity gets modified by the nonlinearity introduced by the external debris as debris velocity increases. This observation also has the similarity with the phenomenon of changing property of the nonlinear wave resulting out of beam-plasma interaction as beam velocity increases [3-5].

*Can other nonlinear phenomena mimic debris-induced nonlinearity?*

We have argued that a high velocity ion beam would behave analogous to an moving external charge debris as long as the ion-acoustic timescale is smaller than the electron-ion collision time ( $\tau_{IA} \ll \tau_{ei}$ ) or beam ions move faster without remaining in phase with plasma waves, thus hindering beam plasma energy transfer process and would affect nonlinear wave dynamics via the electric field, similar to an external charge perturbation.

- Toward this, we observe a resemblance between the DSWs excited by a moving debris in a low negative ion density PINI plasma to the oscillatory IA shocks excited by positive ramp signal in absence of the negative ions [16].
- Similarly, DSWs are observed to be excited by negatively charged debris in a high  $\delta$  plasma when debris velocity crosses the sound speed which are also observed in negative pulse-excited high negative ion density plasma with a positive ion beam [5].
- We have also observed that positively charged debris introduce a positive nonlinearity when the negative ion concentration is low (low  $\delta$ ), while the same debris excites a negative nonlinearity when the negative ion concentration is high (high  $\delta$ ). This phenomenon is similar to what is observed with a positive ion beam in a PINI plasma [3].
- Further the amplitudes of nonlinear waves are observed to increase for both positive and negative perturbation with increase in the debris velocity, which is similar to the case of increasing beam velocity in PINI plasma [4, 5].

### ACKNOWLEDGMENTS

One of the authors, HS thanks CSIR-HRDG, New Delhi, India for Senior Research Fellowship (SRF) research grant 09/059(0074)/2021-EMR-I.

- 
- [1] R. B. White, B. D. Fried, and F. V. Coroniti, Phys. Fluids **15**, 1484 (1972).
  - [2] Y. Nakamura, J. L. Ferreira, and G. O. Ludwig, J. Plasma Phys. **33**, 237 (1985).
  - [3] Y. Nakamura, Plasma Phys. Control. Fusion **41**, A469 (1999).
  - [4] S. K. Sharma and H. Bailung, Phys. Plasmas **17**, 032301 (2010).
  - [5] H. Bailung, S. K. Sharma, and Y. Nakamura, Phys. Plasmas **17**, 062103 (2010).

- [6] R. F. Pfaff, J. E. Borovsky, and D. T. Young, *Geophys. Monogr. Ser.* **102** (1998).
- [7] M. Hirahara, S. Tanaka, H. Kataoka, S. Kasahara, and S. Kubo, *Adv. Space Res.* **72**, 4934 (2023).
- [8] A. Sen, S. Tiwari, S. Mishra, and P. Kaw, *Adv. Space Res.* **56**, 429 (2015).
- [9] S. Jaiswal, P. Bandyopadhyay, and A. Sen, *Phys. Rev. E* **93**, 041201 (2016).
- [10] S. Kumar Tiwari and A. Sen, *Phys. Plasmas* **23**, 022301 (2016).
- [11] A. S. Truitt and C. M. Hartzell, *J. Spacecr. Rockets* **57**, 876 (2020).
- [12] D. Chakraborty, A. Biswas, and S. Ghosh, *Phys. Plasmas* **29** (2022).
- [13] H. Sarkar and M. P. Bora, *Phys. Plasmas* **30**, 083701 (2023).
- [14] K. Kumar, P. Bandyopadhyay, S. Singh, and A. Sen, *Phys. Plasmas* **31**, 023705 (2024).
- [15] M. Das and M. P. Bora, *arXiv e-prints*, arXiv:2402.18478 (2024).
- [16] P. Pathak and H. Bailung, *IEEE Trans. Plasma Sci.*, 1 (2025).
- [17] J. P. Boris and D. L. Book, *J. Comput. Phys.* **11**, 38 (1973).
- [18] S. T. Zalesak, *J. Comput. Phys.* **31**, 335 (1979).
- [19] Y. Nakamura, H. Bailung, and Y. Saitou, *Phys. Plasmas* **11**, 3925 (2004).